

TASK ALLOCATION AND STOP OPTIMIZATION FOR AUTONOMOUS WEEDING

DAVID RAZHIEL CERES ARROYO



A Multi-Tool Allocation Approach for Optimized Weed Removal in Autonomous
Agriculture

June 2025 – classicthesis v4.8

David Razhiel Ceres Arroyo: *Task Allocation and Stop Optimization for Autonomous Weeding, A Multi-Tool Allocation Approach for Optimized Weed Removal in Autonomous Agriculture*, © June 2025

ABSTRACT

Hand weeding has traditionally been a labor-intensive and time-consuming task, making it an ideal candidate for automation. However, fields with high weed density remain a challenge for autonomous systems. In such scenarios, the limited number of robots and their tooling capacities create bottlenecks, leading to extended mission times. Nuga is a more capable system proposed by Paltech to improve throughput efficiency and reduce total mission duration. These benefits, however, depend on effectively solving the task allocation problem with a focus on minimizing tool idle time. To address this, we propose three task allocation algorithms of different paradigms: graph search, optimization-based, and market-based. Our results demonstrate that these approaches can reduce total mission time by up to 22.8% in high-density scenarios and decrease tool idle time by as much as 94.9% in comparison with the baseline method.

*Don't wish it was easier wish you were better.
Don't wish for less problems wish for more skills.
Don't wish for less challenge wish for more wisdom.*

— Jim Rohn

ACKNOWLEDGMENTS

Put your acknowledgments here.

Many thanks to everybody who already sent me a postcard!

Regarding the typography and other help, many thanks go to Marco Kuhlmann, Philipp Lehman, Lothar Schlesier, Jim Young, Lorenzo Pantieri and Enrico Gregorio, Jörg Sommer, Joachim Köstler, Daniel Gottschlag, Denis Aydin, Paride Legovini, Steffen Prochnow, Nicolas Repp, Hinrich Harms, Roland Winkler, Jörg Weber, Henri Menke, Claus Lahiri, Clemens Niederberger, Stefano Bragaglia, Jörn Hees, Scott Lowe, Dave Howcroft, José M. Alcaide, David Carlisle, Ulrike Fischer, Hugues de Lassus, Csaba Hajdu, Dave Howcroft, Anonymous, Konrad Höffner, and the whole L^AT_EX-community for support, ideas and some great software.

Regarding LyX: The LyX port was intially done by Nicholas Mariette in March 2009 and continued by Ivo Pletikosić in 2011. Thank you very much for your work and for the contributions to the original style.

CONTENTS

1	INTRODUCTION	1
1.1	Background and Context	1
1.2	Problem Definition	2
1.3	Related Work	2
1.4	Proposed Solution	5
2	METHODOLOGY	7
2.1	Task Allocation and Optimization	7
2.1.1	Metrics	7
2.1.2	Heuristics	9
2.1.3	Graph Search	11
2.1.4	Optimization	15
2.1.5	Market-based	18
3	RESULTS	23
3.1	The Robot	23
3.2	Simulation	23
3.2.1	URDF	24
3.2.2	SDF	25
3.2.3	Gazebo Plugins	26
3.2.4	Joint Control	26
3.2.5	Localization	28
3.2.6	Weed Detection	28
3.2.7	Nuga Controller	29
3.3	Task Allocation	31
3.3.1	Simulation Setup	31
3.3.2	Algorithm Comparison	31
3.3.3	Computation Time	36
3.3.4	Future Work	37
4	CONCLUSIONS	39
A	APPENDIX	41
A.1	Configuration Files	41
A.2	Algorithms	43
	BIBLIOGRAPHY	45

LIST OF FIGURES

Figure 1.1	Task Allocation classification.	2
Figure 2.1	Problem Layout Dimentions	8
Figure 2.2	Mission Dashboard	8
Figure 2.3	Heuristic Algorithm	10
Figure 2.4	Suboptimal solution computed using Heuristic	11
Figure 2.5	Optimal solution	11
Figure 2.6	Node types and cost representation	12
Figure 2.7	Graph expansion process	14
Figure 2.8	Graph Search Solution	14
Figure 2.9	Cost example of invalid solutions	15
Figure 2.10	Mixed-Integer Programming Solution	18
Figure 2.11	Bidding Mechanism Example	18
Figure 2.12	Market-based Solution	21
Figure 3.1	Nuga Platform	23
Figure 3.2	Simulator Components	24
Figure 3.3	Robot definition using URDF	25
Figure 3.4	Weed Infestation Example	26
Figure 3.5	Implement Tool (IT) Workspace Layout	27
Figure 3.6	ROS Interface for back gantry control	27
Figure 3.7	Example of trainning and detection	29
Figure 3.8	Nuga Controller ROS Interface	29
Figure 3.9	RViz Visualization	30
Figure 3.10	Weed distribution and coverage path in an agricultural field	31
Figure 3.11	Simulation Example	32
Figure 3.12	Low density algorithms comparison	32
Figure 3.13	Medium density algorithms comparison	33
Figure 3.14	High density algorithms comparison	33
Figure 3.15	Graph Search algorithm performance	37

LIST OF TABLES

Table 1.1	Task Allocation approaches (1/2)	3
Table 1.2	Task Allocation approaches (2/2)	4
Table 1.3	Comparison between Task Allocation approaches	5
Table 3.1	Low-density Simulation Results	34
Table 3.2	Medium-density Simulation Results	35

LISTINGS

Listing A.1	Weed Infestation World config example	41
Listing A.2	ROS2 config example	42

ACRONYMS

TA	Task Allocation
SVCA	Shapley Value Clustering Algorithm
CBDTA	Consensus-Based Distributed Task Allocation Algorithm
VDKM	Voronoi Diagram-Based, K-Means Algorithm
CBBA	Consensus-Based Bundle Algorithm
SSI	Sequential Single Item
CBPAEA	Consensus Based Parallel Auction and Execution Algorithm
GRU	Gated Recurrent Units
MLP	Multi-Layer Perceptron
EDACAM	Encoder Decoder Architecture with Cross Attention Mechanism
GNN	Graph Neural Network
PSO	Particle Swarm Optimization Algorithm
MIQP	Mixed-Integer Quadratic Program
STADAA	Sequential Task Addition Distributed Assignment Algorithm
GA	Genetic Algorithm
COQP	Constraint Optimization as Quadratic Program
IT	Implement Tool
DOF	Degrees of Freedom
URDF	Unified Robot Description Format
SDF	Simulation Description Format
WS	Workspace
DFS	Depth-First Search
BFS	Breadth-First Search

MIP Mixed-Integer Programming

1

INTRODUCTION

1.1 BACKGROUND AND CONTEXT

Autonomous systems are complex agents capable of carrying out operations without human intervention. They have become more capable thanks to technological advancements and increasingly integrated into society with recent remarkable progress in artificial intelligence (AI) techniques. According to Zhang in [1], current trends indicate that the development and adoption of such systems will continue to grow in the coming years.

The agricultural sector is one of the areas where the integration of autonomous technologies has great potential. These systems could significantly benefit farmers by making their work safer and less repetitive. Autonomous systems have already been used in alternative cropping methods such as precision agriculture. Nevertheless, traditional practices are still facing challenges that autonomous systems could perfectly address. Among these challenges, the proliferation of weeds in grass fields raises as a major concern for the livestock well-being for two main reasons. First, weeds compete with grass for resources, causing forage loss [2]. Second, some weed species pose a direct threat to livestock health. In particular, plants like Herbstzeitlose (*Colchicum autumnale*) have been identified as toxic and the cause of livestock poisoning [3].

Removing these plants is a task that organic farmers must perform manually, as EU regulations restrict the use of pesticides and prevent farmers from combating weed proliferation through chemical means. It is evident that this task, especially in large grass fields, is highly time-consuming and extremely repetitive, making it an ideal candidate for automation. In Germany, companies like Paltech have developed solutions to address this problem using autonomous wheeled robots. Their flagship robot is a differential-drive wheeled system equipped with various sensors for localization and weed detection, as well as an onboard mechanism for weed removal. Currently, if the weed removal process needs to be sped up, the only solution is to deploy a fleet of robots. While this is feasible, developing single units capable of holding more than one weed control mechanism seems like the natural next step in Paltech's solution.

1.2 PROBLEM DEFINITION

The development of systems with more than one mechanism for weed removal comes with both hardware and software challenges. It is crucial to ensure that tools and system resources are used as efficiently as possible. Paltech wants to avoid having more capable units with unused tools, especially since the production and deployment of these improved systems are more costly. Therefore, reducing idle time is a top priority and the focus of this thesis.

Idle time refers to periods when resources, such as tool equipment, are not actively engaged in productive work. Reducing idle time in this context means minimizing the time tools remain unused and maximizing their productivity in weed removal. To achieve this, allocating detected plants to the correct tools is essential. In the literature, this process is known as Task Allocation (TA). Some technical challenges to consider during implementation include computational latency and multi-tool coordination. The TA algorithm and execution pipeline must be fast enough to process new detections and reassign tools in real time without causing delays, while also ensuring that multiple tool units operate efficiently without interference or redundancy.

1.3 RELATED WORK

In general, a TA system aims to achieve an efficient assignment of tasks to robots (or tools in this case) by considering various characteristics such as the robots' capabilities, task requirements, and system efficiency. This process of TA involves three important factors to be considered according to Umashankar in [4]. Robot/tool, environment and coordination as shown in Figure 1.1.

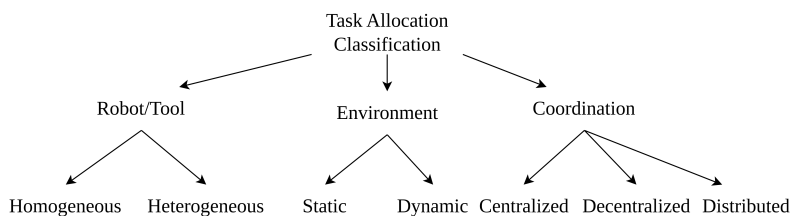


Figure 1.1: Task Allocation classification.

An example of homogeneous tools in this context is a robot equipped with multiple tools of the same type, such as drills. In contrast, heterogeneous tools refer to robots equipped with different types of tools, such as drilling, seeding, and sensing equipment.

The multi-tool TA can take place in either a dynamic or static environment. In an environment that is static in nature, tasks are allocated to tools in advance before they begin to execute them. This method works well in situations when the tasks are predetermined and the

environment remains unchanged. In contrast, dynamic TA involves the real-time assignment of tasks to tools as they carry out their activities. For the scope of this thesis, we will focus on homogeneous tools operating in a dynamic environment with centralized coordination, where the onboard computer will act as the master, assigning plants to each weed control mechanism.

There are several ways to accomplish multi-tool allocation, including heuristic, cluster-based, market-based, learning-based, and optimization-based techniques. Table 1.1 and 1.2 presents a comprehensive classification of TA algorithms found in the literature [4].

APPROACH	TECHNIQUE / ALGORITHM
Cluster Based	SVCA [5]
	Group Agent Partitioning [6]
	CBDTA [7]
	VDKM [8]
	CBBA [9]
Market Based	K-Means Clustering [10]
	Auction Algorithm [11]
	Improved Auction Algorithm [12]
	SSI Auction Algorithm [13]
	Extended SSI [14]
	Multihop-Based auction Algorithm [15]
	CBPAEA [16]
	Distributed Auction-Based Algorithm [17]

Table 1.1: Comparative overview of cluster-based and market-based approaches to Task Allocation.

In cluster-based approaches, the goal is to group tasks into a predefined number of clusters. Instead of assigning a single task to each tool, the clustering approach allocates entire groups of tasks to them, reducing the number of individual task assignments and computational complexity. Clustering approaches aim to minimize travel distance and maximize task coverage by grouping tasks effectively. However, the optimal clustering of tasks still needs further exploration. Although these approaches simplify TA, they struggle to handle dynamic changes in the environment.

An optimization-based strategy aims to select the best solution from a set of available options. These solutions are constrained by specific conditions, and the optimal one is determined based on the objective function. The objective function represents the system's ultimate goal. Some of the optimization algorithms have poor robustness

APPROACH	TECHNIQUE / ALGORITHM
Learning Based	GRU, MLP [18]
	Deep Reinforcement Learning [19]
	Heterogeneous Graph Attention Network [20]
	Capsule Attention-Based Mechanism [21]
	EDACAM [22]
	Graph Neural Network (GNN) [23]
Optimization Based	Mixed-Integer Quadratic Program [24]
	STADAA [25]
	PSO [26]
	Integer Programming [27]
	MIQP [28]
	Genetic Algorithm (GA) [29]
	COQP [30]
	Heuristic Based [31]
	Fuzzy Optimization [32]

Table 1.2: Comparative overview of learning-based and optimization-based approaches to Task Allocation.

to uncertainties therefore this approach is more suitable for solving well-defined and static problems focusing on theoretically optimal or near-optimal solutions. Additionally, optimization-based approaches require more computational power and are less adaptable to changing environments.

Market-based approaches effectively handle highly combinatorial optimization problems. In this method, an auctioneer informs agents about available tasks and requests bids. Each agent evaluates its capacity to complete the tasks and submits a bid accordingly. The auctioneer then assigns tasks to the agent with the most favorable bid. Generally, TA using this approach minimizes travel time. While these methods are flexible and scalable, they may not always achieve a globally optimal solution.

Recent approaches to TA incorporate deep learning techniques such as graph neural networks and graph convolutional networks. These types of TA methods are commonly referred as learning-based approaches. Most learning-based approaches struggle to generalize to larger-scale problem scenarios beyond those used during training. This characteristic is especially important because real-world TA problems frequently require modeling scenarios whose costs increase with the number of tasks and robots. Table 1.3 gives a comparison between all the approaches, Source [4].

	Clustering	Optimization	Market	Learning
Advantage	Simplifies TA and reduces complexity	Provides optimal solutions, suited for static problems	Flexible, scalable, decentralized	Adaptable, learns, and improves over time
Limitation	May not account for dynamics well	Computationally intensive, less adaptable	May not be global optima, needs effective bidding	Requires training, initially sub-optimal
Best case	Logical tasks	Well-defined, static problems	Dynamic environments with varying tasks	Complex and uncertain environments
Future work	Dynamic clustering, online adaptation	Hybrid models, real-time optimization	Adaptive market mechanisms, incentive models	Transfer learning, meta-learning

Table 1.3: Comparison between Task Allocation approaches

1.4 PROPOSED SOLUTION

As Table 1.3 illustrates, algorithm selection must be carefully considered based on the application's nature to achieve optimal performance. In a grass field clearing application, the environment is highly dynamic, especially since weed detections occur while the system is in motion. Therefore, market-based approaches are well-suited to ensuring the system adapts effectively to such conditions. However, this solution might not be optimal.

Optimization-based solutions, on the other hand, are known for providing optimal results, but they are typically more suited for static problems. In our case, although the environment is dynamic, this approach is still worth exploring. Since tasks are continuously added and removed from the allocation problem, the computation time at this task density may not be a significant issue, making real-time optimization feasible.

A graph search approach is also proposed, which becomes particularly interesting if the problem can be translated into a graph representation. Using well-known algorithms such as Depth-First Search ([DFS](#)) [33] or Dijkstra's [34] can help find the lowest-cost solution and achieve effective resource allocation, reducing both idle time and overall mission duration.

Lastly, clustering and learning-based approaches will be discarded. Clustering due to the challenges of dynamic clustering and the need for online adaptation. Although it offers the advantage of simplifying [TA](#), its benefits diminish in low to medium density scenarios. Learning-based approaches are excluded because of the required training phase and the difficulty of generalizing across environments with varying task densities.

2

METHODOLOGY

2.1 TASK ALLOCATION AND OPTIMIZATION

Solving the **TA** problem in this context means assigning weed detections to removal tools in the most efficient way. The idea is to find the best allocation of resources and the optimal sequence of stops, that will maximize the number of plants removed, and minimize the tools' idle time. The solution has to consider the constraints of the problem such as:

GEOMETRIC CONSTRAINTS: A stop is considered valid only if the weeds lie within the workspaces of the tools (observe [Figure 2.1](#)).

MOVEMENT CONSTRAINTS: The robot can only move forward in a straight line at a max speed of $0.3 \frac{m}{s}$.

TASK PROCESSING: Each plant removal takes approximately 45 seconds, during which the robot must remain stationary to ensure a successful extraction. Movement during this process is not allowed as it could compromise the tool operation.

DYNAMIC ENVIRONMENT: Weed positions are initially unknown and are discovered dynamically during operation by the camera in front of the vehicle.

PROCESSING TIME: The solution must run online because the robot discovers new weeds during operation, and decisions about stopping and **TA** must adapt in real-time.

We define a '*good*' stop as the next robot position that maximizes plant coverage while keeps a balance on the number of tasks assigned to each implement (aiming to minimize idle time). The problem can be approached in two ways: one option is to first determine the optimal stop location, after which **TA** is solved over the reachable tasks. Alternatively, we can first allocate tasks to the implements and then compute the stop position that satisfies the corresponding geometric constraints. Both approaches are similar, differing mainly in the order of operations, but each perspective opens the door to different methods and algorithms to try.

2.1.1 Metrics

Defining a good set of metrics is crucial to establish a solid basis for comparison between solutions and to easily identify the flaws of

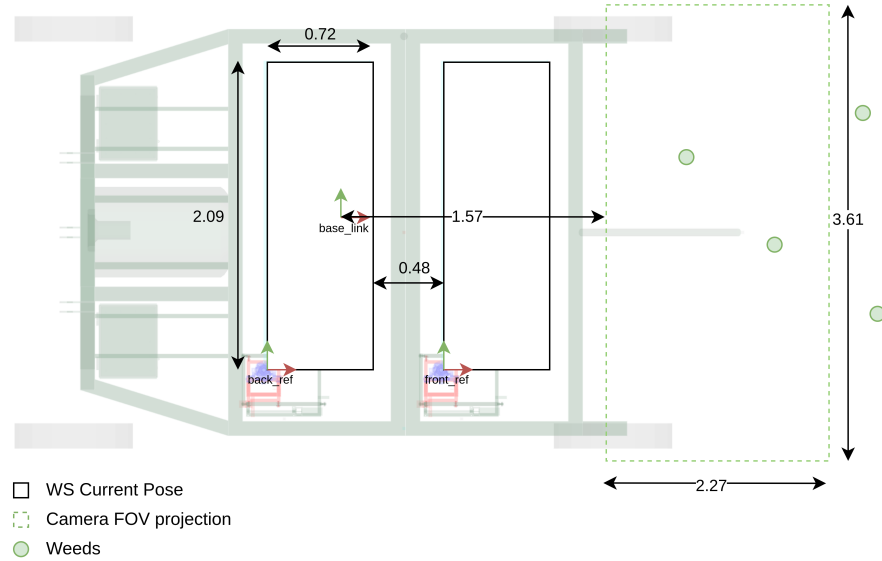


Figure 2.1: Problem Layout Dimensions

each method, thereby determining the best solution. To address this, we define two main categories. The first summarizes mission-level metrics such as the total idle and productive time of each tool, and the total time the robot spends moving or in a stationary state (defined by equations 2.1 and 2.2). The second category includes task-specific information, for example, task ID, status ('completed', 'failed', 'out'), number of stop, the tool that processed the task, and the idle and productive time of each tool at that specific stop. These metrics are displayed in a mission dashboard for easy visualization and comparison across missions using different scenarios or algorithms (see Figure 2.2b for the first category and 2.2a for the second one).

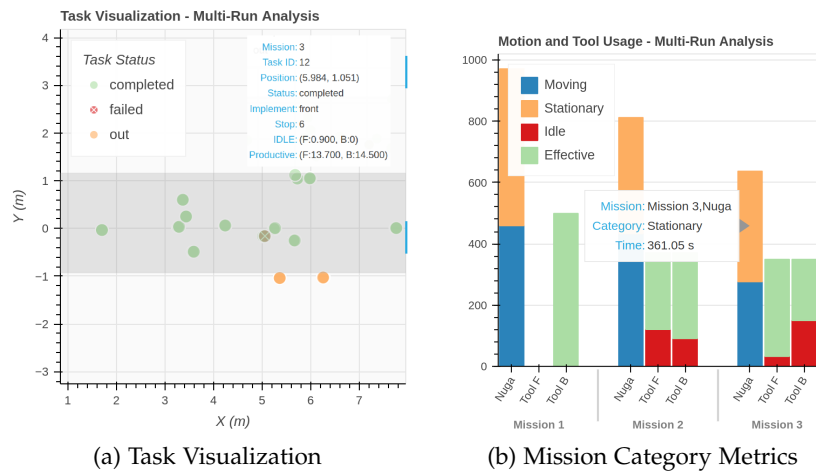


Figure 2.2: Mission Dashboard

FIGURE 2.2A Displays a 2D grid of the removed tasks' positions during the mission, along with their corresponding metadata. Hovering over a task reveals its details, and tasks can be filtered by mission.

FIGURE 2.2B Showcases a bar graph comparing different missions. Each mission includes the robot's moving and stationary time, as well as the idle and productive time of the onboard implement tools. A hover feature displays the value of each category.

$$t_{mission} = t_{moving} + t_{stationary} \quad (2.1)$$

$$t_{tool_operation} = t_{idle} + t_{productive} \quad (2.2)$$

2.1.2 Heuristics

Heuristic solutions are commonly employed when the solution space of an optimization problem is too large to explore exhaustively, making an exact optimal solution computationally infeasible. They are also useful in time-sensitive scenarios, such as online implementations, where sacrificing optimality for efficiency is often justified.

In our work, we developed a heuristic algorithm to serve as a baseline solution, this provides a meaningful reference point to assess the performance and potential improvements offered by other algorithms. The algorithm' description is detailed in 1, with an illustrative example in Figure 2.3.

Algorithm 1 Heuristic

- 1: Get the position of the closest weed from the current robot position.
 - 2: Project the tools' Workspace (WS) forward (in the future), aligning the trailing edge of the last WS with the closest weed's position plus a small clearance (e.g., 10 cm).
 - 3: Allocate weeds to each tool if they fall within its projected WS.
 - 4: Move the robot until the tools' WS are aligned with their projections, then execute the extractions for tools with assigned weeds.
 - 5: Repeat the process until mission has ended.
-

This approach offers a simple implementation and fast computation solution, making it well-suited for online applications. However, its heuristic nature leads to suboptimal solutions, as it does not account for minimizing idle time. In Figure 2.4 we exemplify the algorithm' suboptimality for a particular case, contrasting with a better solution to support our analysis.

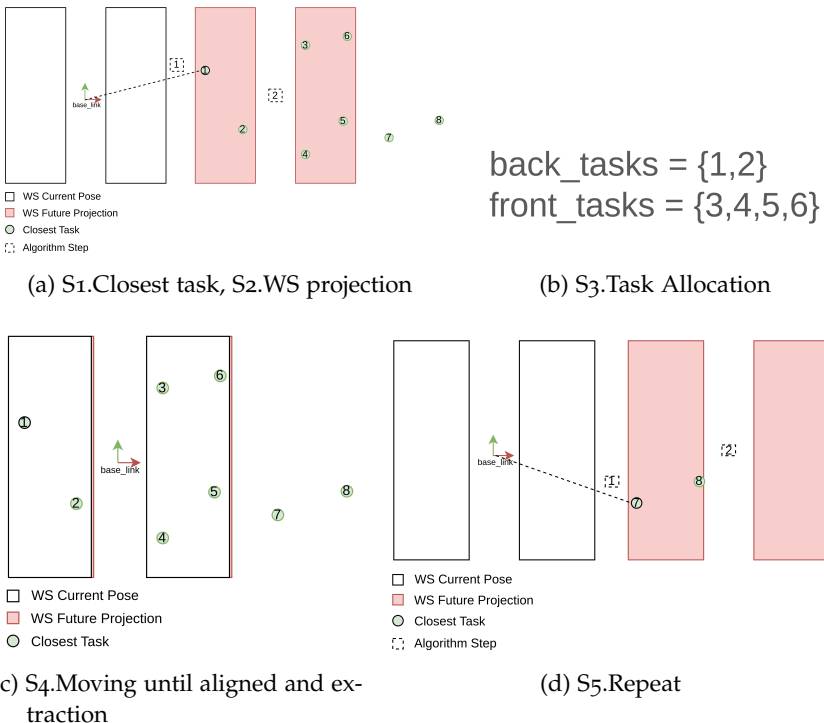


Figure 2.3: Heuristic Algorithm

FIGURE 2.4A Showcases the two stops required to remove eight detected weeds, with the first stop allocating four tasks to the back tool and two to the front, the second stop allocates remaining two tasks in the back.

FIGURE 2.4B Illustrates the idle and productive time for the given solution. Blue represents the robot's repositioning time, red indicates the idle time of the respective tool, and white the productive time. The first stop shows a significant idle time for the front tool (90 seconds, equivalent to two tasks), caused by the tool waiting for the back tool to finish before proceeding to the next stop. The second stop shows a similar situation, where idle time arises from the only feasible option at that point: removing tasks 5 and 6 with the back tool.

An alternative solution for the same scenario (this time aimed at reducing idle time) is illustrated in [Figure 2.5](#). In this case, the solution requires three stops: first stop assigns tasks 1 to back tool and task 5 to the front, the second stop processes tasks 2 and 6, and finally the third stop is used to remove tasks 3, 4, 7, and 8. As shown in [Figure 2.5b](#), the balanced TA between tools eliminates idle time and reduces the total mission duration compared to the previous solution.

This demonstrates the heuristic's suboptimality, as it fails to minimize idle time and does not consider the possibility of stopping at a location that allows for a more efficient TA. The heuristic algorithm is limited to the closest weed detection, which may not always be the best option.

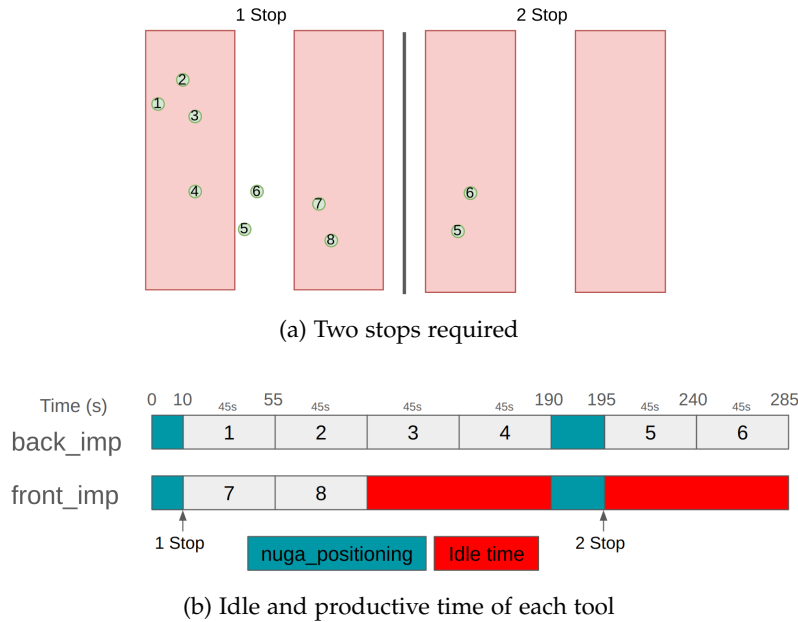


Figure 2.4: Suboptimal solution computed using Heuristic

In the following sections, we will explore more sofisticated algorithms that can overcome these limitations and provide better solutions.

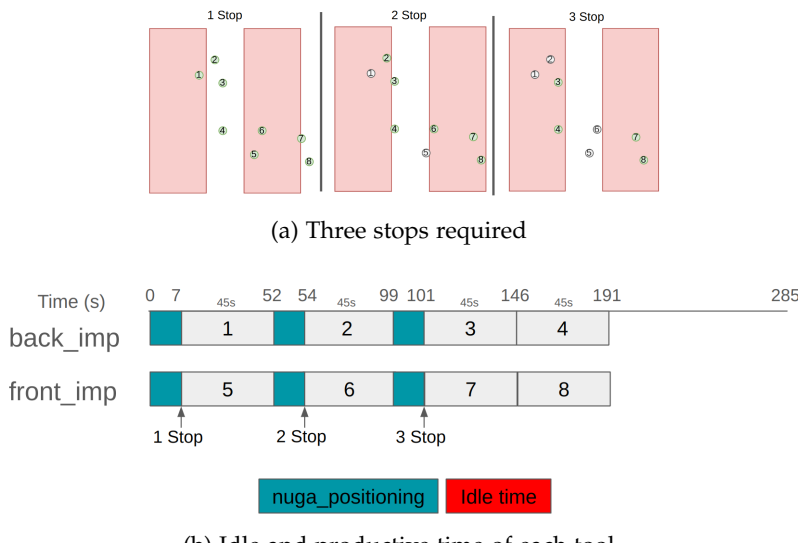


Figure 2.5: Optimal solution

2.1.3 Graph Search

Graph Search are a type of algorithms widely used in graph theory to systematically explore or traverse a graph. They are commonly used to find the shortest path between nodes, identify connected components, or solve various optimization problems. Graph search algorithms can

be broadly categorized into two main types: uninformed and informed search algorithms.

Uninformed search algorithms do not have any additional information about the problem domain and explore the graph blindly. Examples include [DFS](#) and Breadth-First Search ([BFS](#)). These algorithms are typically used for tasks like finding connected components or traversing all nodes in a graph. Informed search algorithms, on the other hand, use heuristics or additional information to guide the search process. They are often more efficient than uninformed algorithms for specific problems. Examples include A* search and Dijkstra's algorithm, which are commonly used for finding the shortest path in weighted graphs.

In our context, we exploit the advantages of graph-based algorithms by modeling the problem as such. Nodes represent potential stop locations, where two types of actions are possible: moving to another stop (a *stop node*) or performing weed removal at that location (an *action node*). Edge weights are defined as follows: edges between two *stop nodes* represent *travel cost*, computed using the distance between stops and the robot's velocity or a unitary value as a placeholder. Edges connecting a *stop node* to an *action node* represent *task execution cost*, and it is calculated based on the idle time (if any) of removing the indicated weeds with the assigned tools.

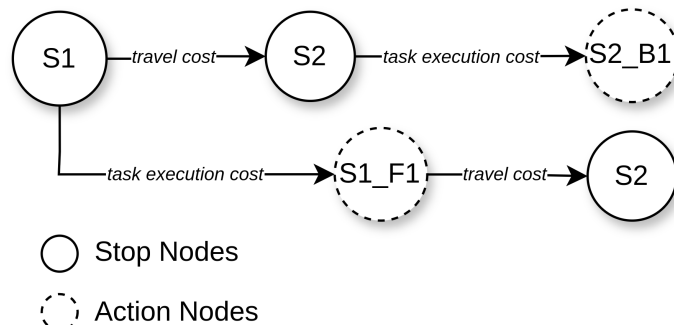


Figure 2.6: Node types and cost representation

FIGURE 2.6 Illustrates the convention used to represent the graph. S1 denotes stop number 1, while F or B indicate whether the front or back tool is assigned to remove the weed, followed by the weed ID to be processed. In this example, the task execution cost between S1 and S1_F1 would be 45s, as the back tool must wait for the front tool to process 1 plant. The same logic applies to the cost between S2 and S2_B1 but for the front tool.

The graph search implementation solution follows the next pipeline:

1. Compute **candidate stops** based on the robot's current position and weed detections. Candidate stops are the locations where

an important event occurs, such as a weed entering or exiting the workspace of a tool.

2. Associate reachable weeds with candidate stops. This allows the algorithm to determine which weeds can be removed at each stop.
3. Create a **graph representation** of the problem using [DFS](#) algorithm and the convention described in [Figure 2.6](#). The graph is built by connecting *stop nodes* and *action nodes* using appropriate edge costs, taking into account the predefined associations between stops and tasks.
4. Get the **shortest path** in the graph from the root (first stop) to the final node (last stop) using Dijkstra's algorithm.
5. **Decode solution** and return the next optimal stop and [TA](#) as the algorithm's output.

To build and explore the graph, an implementation of the [DFS](#) algorithm is used (see Algorithm 4). The `get_children_nodes` method expands the graph by generating child nodes from a given parent node. If the parent node is a *stop node*, it creates child nodes for all valid combinations of reachable tasks that can be processed at that stop. Each combination forms a new child node that reflects the state after removing those tasks (*action node*). Additionally a 'trivial' *stop node* is added representing the decision to move to the next stop without removing any weeds. On the other hand, if the parent node is an *action node*, this method creates a single *stop node* representing the next stop. Each created edge is added to the graph with a weight based on the associated *task execution cost* or *travel cost*. [Figure 2.7](#) illustrates the graph expansion process, where the algorithm grows all possible combinations of tasks at each stop and generates the corresponding child nodes.

We observe that from S3 four possible states can be reached (three *action nodes* and one *stop node*). The transition S3_B1_F2 achieves zero idle time by optimally balancing tasks between the front and back tools, whereas the other transitions result in higher idle times due to imbalanced assignments. It's important to note that the same stop can be reached through different paths, depending on the actions taken at previous stops. For instance, if task 1 has been removed earlier, it should no longer be considered in subsequent stops. This consideration is crucial when building the graph, as we must ensure that it is expanded only through valid and realistic transitions that reflect feasible execution scenarios.

Having the complete graph, and given its configuration as a weighted directed graph, we choose Dijkstra's algorithm to find the optimal path. This algorithm efficiently explores the graph by maintaining a priority queue of nodes to be processed, ensuring that the node with

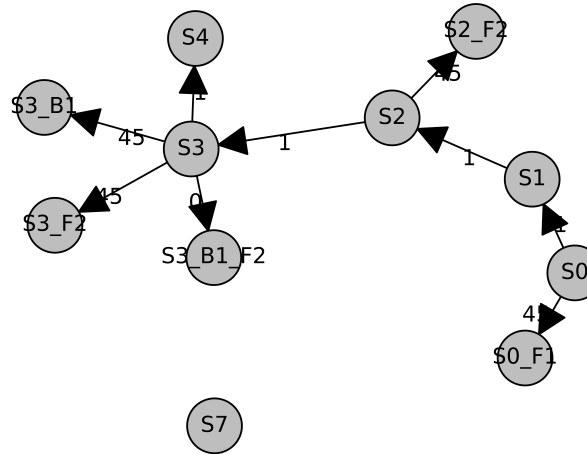


Figure 2.7: Graph expansion process

the lowest cost is always explored first. The algorithm continues until it reaches the final node, which represents the optimal solution. The path is then traced back from the final node to the root, revealing the sequence of stops and actions that lead to the optimal solution.

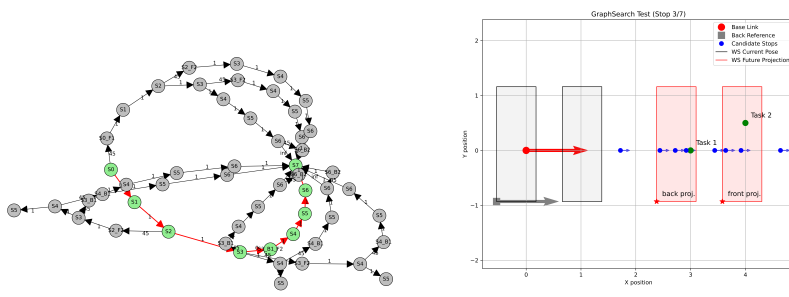
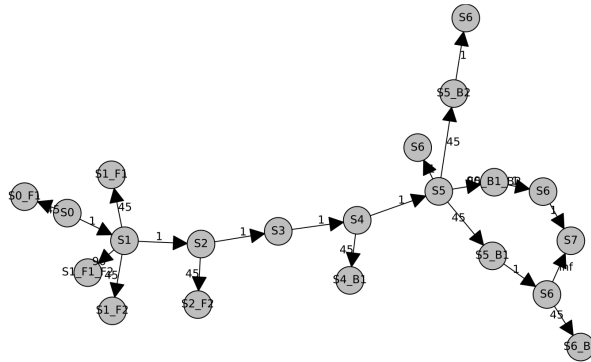


Figure 2.8: Graph Search Solution

An optimal solution obtained by the graph search algorithm in a scenario with two detected weeds is illustrated in Figure 2.8a. The highlighted branch corresponds to the optimal path found by the algorithm. For the given two weeds, the graph contained 54 nodes, and the computation time was 0.001 seconds. A visual representation of the solution is shown in Figure 2.8b, including the current robot pose, projected workspaces in red, candidate stops in blue, and weeds in green.

One remaining issue to address is preventing the algorithm from returning trivial solutions in which either no weeds are removed or not all of them are. To tackle this, each node keeps track of the tasks completed so far. If, at the second-to-last node, there are still tasks left to remove, we assign a penalty cost to the edge leading to the final node. This encourages the algorithm to prioritize removing all

weeds before proceeding to the last stop. An example is presented in [Figure 2.9](#). Notice that there are two branches connecting nodes S_0 and S_7 , but only one is feasible. The invalid branch includes a segment between S_6 and S_7 with a cost of 'inf', indicating that this solution removes fewer weeds than the available. By repeating this check as the graph grows, the algorithm only returns solutions where all tasks are removed.



[Figure 2.9](#): Cost example of invalid solutions

Although the graph search algorithm is a promising approach, it still suffers from the exponential growth of the graph size as the number of weeds increases (as discussed in [Section 3.3.3](#)). This can lead to longer computation times and may not be suitable for real-time applications with high weed densities. In the next section, we will explore optimization-based approaches that can potentially overcome these limitations and provide more efficient solutions.

2.1.4 Optimization

As discussed at the beginning of this chapter, the main goal of [TA](#) is to find the best allocation of resources and the optimal sequence of stops while considering the given constraints. Achieving such a solution requires mathematically formulating the scenario as an optimization task, with a clearly defined objective function, set of constraints, and decision variables that fully describe the problem. Optimization-based approaches are powerful tools that provide a systematic way to find the best feasible solution to a problem by exploring the solution space. Depending on the nature of the problem, a different optimization formulation can be used, such as linear programming, Mixed-Integer Programming ([MIP](#)), or nonlinear programming. In our case, we will focus on [MIP](#) as the most suitable approach for the problem.

[MIP](#) is a mathematical optimization technique that combines both integer and continuous variables in the formulation of the problem. It

allows for the modeling of complex decision-making scenarios where some variables must take on discrete values (e.g., binary decisions) while others can take on continuous values. This flexibility makes MIP particularly useful for problems that involve resource allocation, scheduling, and other combinatorial optimization tasks.

Given a set of tasks $\mathcal{T} = \{1, 2, \dots, T\}$ where each task $j \in \mathcal{T}$ corresponds to one weed detection from a total T , and a set of candidate stops $\mathcal{S} = \{1, 2, \dots, S\}$ where each stop $i \in \mathcal{S}$ is computed using events as in Graph Search algorithm. Let $x_{i,j} \in \{0, 1\}$ be a binary decision variable equal to 1 if task j is assigned to stop i , 0 otherwise and $imb_i \in \mathbb{N}_0$ the imbalance of assigned tasks between tools at stop i . We know that from each stop i we can only assign tasks that are visible from that stop, and a subset for those corresponds to tasks set to front or back tools, these statements could be better defined as:

- $\mathcal{V}_i \subseteq \mathcal{T}$ Set of tasks visible from stop i
- $\mathcal{F}_i \subseteq \mathcal{V}_i$ Front tool task assigned at stop i
- $\mathcal{B}_i \subseteq \mathcal{V}_i$ Back tool task assigned at stop i
- τ Constant processing time per task

We know that each task must be assigned to exactly one stop.

$$\sum_{i=1}^S x_{i,j} = 1 \quad \forall j \in \mathcal{T} \quad (2.3)$$

While visible tasks can only be assigned its corresponding stops.

$$x_{i,j} = 0 \quad \text{if } j \notin \mathcal{V}_i \quad (2.4)$$

The imbalance per stop is the absolute time difference between front and back tools.

$$f_i = \sum_{j \in \mathcal{F}_i} x_{i,j} \quad \text{and} \quad b_i = \sum_{j \in \mathcal{B}_i} x_{i,j} \quad (2.5)$$

We want the imbalance imb_i to reflect the time difference between front and back processing times at each stop. Therefore, we define the imbalance as the maximum of the two possible differences.

$$|\tau(f_i - b_i)| = \max(f_i - b_i, b_i - f_i) \quad (2.6)$$

Thus

$$imb_i \geq \tau(f_i - b_i) \quad \text{and} \quad imb_i \geq \tau(b_i - f_i) \quad (2.7)$$

Or equivalently

$$imb_i \geq |\tau(f_i - b_i)| \quad \forall i \in \mathcal{S} \quad (2.8)$$

The objective function is to minimize the total idle time, expressed as follows

$$\min \sum_{i=1}^S imb_i \quad (2.9)$$

Given the constraints and objective function, we can formulate the optimization problem as follows:

$$\begin{aligned} & \text{minimize} && \sum_{i=1}^S imb_i \\ & \text{subject to} && \sum_{i=1}^S x_{i,j} = 1 \quad \forall j \in \mathcal{T} \\ & && x_{i,j} = 0 \quad \text{if } j \notin \mathcal{V}_i \end{aligned} \quad (2.10)$$

An advantage of an optimization-based approach is that once the problem is formulated we can use existing optimization libraries to obtain the solution. In our case, we used the Google OR-Tools¹ library to solve our combinatorial problem.

The pipeline for the optimization-based approach is as follows:

1. Compute **candidate stops** based on the robot's current position and weed detections.
2. **Associate** reachable weeds with candidate stops.
3. Build the **optimization model** using decision variables, constraints, and objective function.
4. **Call solver** to get solution.
5. **Decode solution** and return the next optimal stop and **TA** as the algorithm's output.

This method does not suffer from high processing times as weed density increases. The algorithm consistently returns a solution in less than 0.1 seconds across a range of weed densities, from low to extremely high (tested up to 6.25 weeds/m²), making it a strong candidate for real-time applications. The optimization model effectively balances tasks between tools while minimizing idle time. [Figure 2.10](#)

¹ OR-Tools is an open source software suite for optimization, tuned for tackling the world's toughest problems in vehicle routing, flows, integer, linear, and constraint programming. <https://developers.google.com/optimization>

illustrates an example of the solution generated by the optimization algorithm in a scenario with twenty weeds.

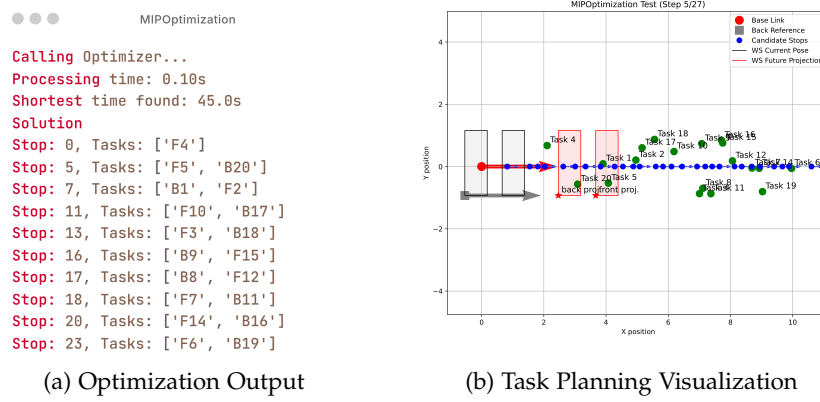


Figure 2.10: Mixed-Integer Programming Solution

2.1.5 Market-based

Market-based approaches are a class of algorithms that leverage the principles of supply and demand to solve TA problems. In our context, we consider the set of visible tasks from each candidate stop ($\mathcal{V}_i \subseteq \mathcal{T}$). Given these tasks, the algorithm forms all possible combinations of allocations and generates a bid for each one. The allocation is then determined based on the bids received and selecting the best one. A ‘*better bid*’ is defined as the combination that maximizes the number of removed weeds while minimizing the imbalance between tools (i.e., idle time). An illustrative example of the bidding mechanism is shown in Figure 2.11.

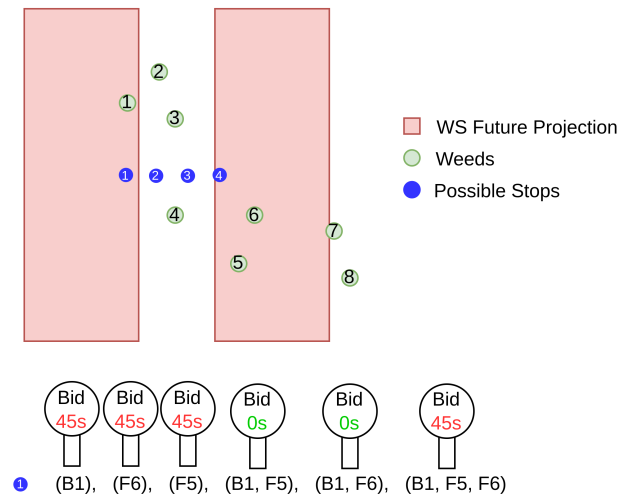


Figure 2.11: Bidding Mechanism Example

FIGURE 2.11 Illustrates a scenario with eight weed detections. The projected future workspace is marked in red and is positioned as if the robot were placed at candidate stop 1. Subsequent candidate stops are marked with blue circles. All possible TA combinations for the first stop are shown, each with its corresponding bid. The best bid is minimizing tool idle time while maximizing the number of removable tasks. This process is repeated for all stops, and the stop with the best overall bid is selected as the winner.

The algorithm is designed to be fast and efficient, making it suitable for real-time applications. Nevertheless, since the approach always selects the best next stop, it falls into the category of greedy algorithms due to its shortsighted nature. In some cases, it is necessary to sacrifice productivity at the next stop to benefit the overall solution, as illustrated in Figure 2.4 and Figure 2.5. The main advantage of this approach is its ability to adapt to dynamic environments where tasks change over time.

The next stop computation follows a similar pipeline to previous algorithms, with the main differences being the use of a bidding process to determine the best solution and the computation of candidate stops. Algorithm 2 outlines the steps involved during the algorithm.

Algorithm 2 Run Algorithm (Market-Based)

Require: Current tasks and robot pose
Ensure: Best stop and task assignment with shortest idle time

```

1: candidate_stops ← get_candidate_stops()
2: associate_tasks_with_stops(candidate_stops)
3: if log_print then
4:   log("Collecting Biddings...")
5: end if
6: start_timer()
7: (stop, tasks, idle_time) ← get_best_bid()
8: sw_time ← stop_timer()
9: if log_print then
10:  log("Processing time: " sw_time"s")
11:  log("Shortest time found: " idle_time"s")
12: end if
13: return (stop, tasks, idle_time)

```

The candidate stops are computed by considering only the closest weed detection and the events this task generate within the back tool workspace. These events include:

1. Entering the workspace.
2. The stop position where the weed is about to exit (rather than when it fully exits).

Using these two candidate poses, we generate evenly distributed positions to create additional candidates between these two events. Afterwards, we perform task association per stop as usual and call `get_best_bid` to start the bidding process and obtain the solution. The algorithm iterates through all possible combinations of tasks at each stop, calculating the idle time for each combination. The combination with the lowest idle time and more number of weeds is selected as the best bid. This process is repeated for all candidate stops, and the best overall stop and `TA` are returned (observe Algorithm 3).

Algorithm 3 Get Best Bid

Require: Candidate stops with associated tasks
Ensure: Best stop and task assignment with minimum idle time

```

1: bid ← Bid( $\emptyset, \infty$ )
2: stops ← []
3: best_stop ← None
4: best_bid ← None
5: for  $i, \text{stop} \in \text{enumerate(candidate_stops)}$  do
6:   tasks_per_stop ← []
7:   for task ∈ stop["tasks"] do
8:     tasks_per_stop.append(task)
9:   end for
10:  combinations ← get_all_combinations(tasks_per_stop)
11:  idle ← get_idle_per_combination(combinations)
12:  bid ← get_bid(zip(combinations, idle))
13:  if update_bid_if_better(bid) then
14:    best_stop ← i
15:    best_bid ← bid
16:  end if
17: end for
18: return stops[best_stop], best_bid.tasks, best_bid.idle

```

An example of the solution produced by this algorithm is illustrated in Figure 2.12. We can observe that only four candidate stops are generated for four tasks. Notice the contrast with the graph search in Figure 2.8b and the optimization approach in Figure 2.10b.

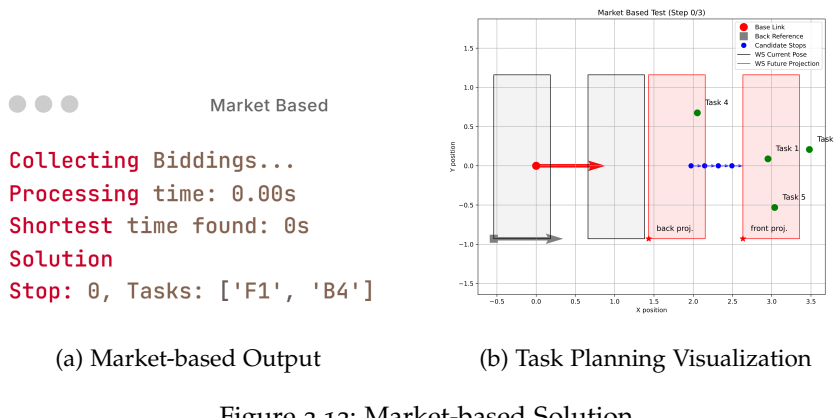


Figure 2.12: Market-based Solution

RESULTS

This chapter presents a detailed explanation of how the simulation was built and a performance comparison of all proposed **TA** methods across different scenarios ranging from low to high weed density. The goal is to identify the most effective solution to the **TA** problem and quantify the performance improvements over the baseline method. Additionally, this chapter clarifies key implementation details and evaluation metrics.

3.1 THE ROBOT

Nuga is Paltech's solution for speeding up the weed removal process. Nuga is a mobile platform equipped with two weed control mechanisms, also called **IT**, one main camera at the front for plant detection, two internal cameras for fine adjustment during tools' placement, an IMU, and two GNSS antennas for GPS localization. Each **IT** is mounted on a structure with three Degrees of Freedom (**DOF**) using prismatic joints, allowing movement in X, Y, and Z directions.

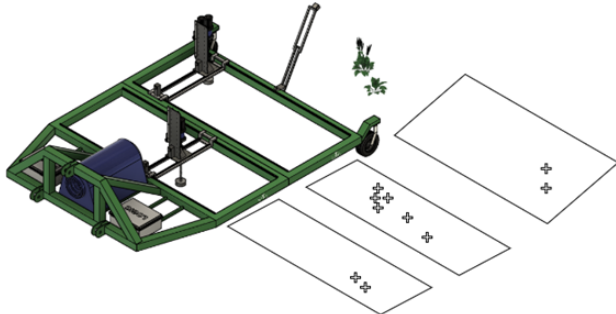


Figure 3.1: Nuga Platform

3.2 SIMULATION

A representative simulation of reality is crucial for developing new algorithms and analyzing robot behavior before real-world implementation. Therefore, building a simulation of the project was a foundational step for this work, ensuring a controlled environment for validation and testing. Gazebo¹ was the selected tool because it pro-

¹ Gazebo is a physics-based robotics simulation tool that allows testing and validation of robot models before real-world deployment. <https://gazebosim.org/home>

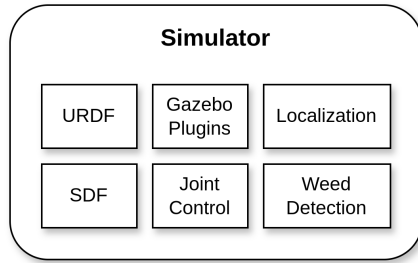


Figure 3.2: Simulator Components

vides a physics engine, supports sensor and actuator modeling, and integrates well with ROS², making it ideal for testing robotic systems.

The simulation consists of six key components: URDF files define the robot's structure and properties, SDF files describe the virtual environment, and Gazebo plugins provide additional functionality, such as simulating custom sensors, actuators, or control interfaces. Additionally, core system operations include joint control for managing the movement of the IT, localization for tracking the robot's position, and weed detection, which relies on an AI model for Rumex recognition. Figure 3.2 illustrates these components as building blocks for the simulation.

3.2.1 URDF

Unified Robot Description Format (URDF) is an XML file used to describe multibody systems for robot simulation. It defines the visual, collision, and inertial properties of rigid body objects, as well as their connections (*joints*). This establishes a spatial relationship between frames, which ROS and Gazebo can later interpret for control and visualization. This file also allows modeling different types of sensors and incorporating Gazebo plugins to link it with ROS control actions. We exploit these capabilities to define camera intrinsics, IMU behavior, GPS properties, and control the IT using `ros2_control`³.

Figure 3.3a displays the structure of the URDF files, being nuga the highest level entity that joins the robot description, gazebo sensor modeling and plugins, as well as `ros2_control` configuration. Nuga description defines the robot's physical structure, including its links (e.g., chassis, wheels, camera support), joints (fixed, continuous, prismatic connections), sensors (cameras, IMU, GPS), and inertial properties. It organizes these components into a kinematic tree

² ROS (Robot Operating System) is an open-source framework that provides tools, libraries, and conventions for developing, managing, and simulating robotic applications. <https://www.ros.org/>

³ `ros2_control` is a ROS 2 framework that provides a standardized interface for managing hardware, enabling modular and reusable control systems for robots. https://control.ros.org/rolling/doc/getting_started/getting_started.html

(e.g., base_link -> chassis_link -> wheels/sensors) using macros for modularity, and resulting in the model displayed in [Figure 3.3b](#).

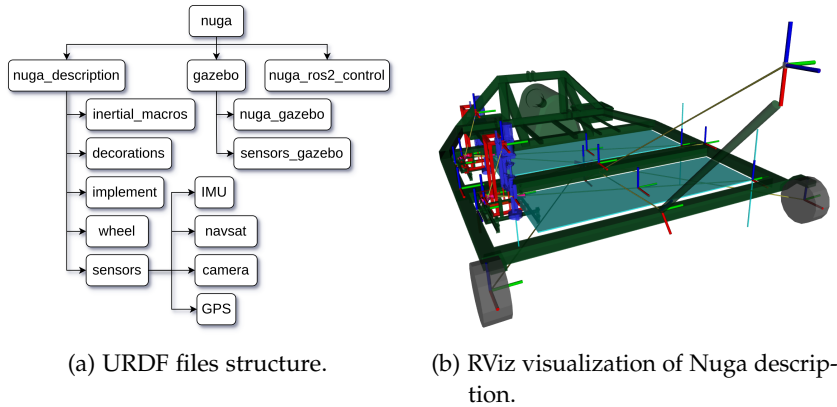


Figure 3.3: Robot definition using URDF

3.2.2 SDF

Simulation Description Format ([SDF](#)) also written in XML, describes the properties of the virtual world. Gazebo uses this file to define the terrain, obstacles, lighting conditions, physics parameters, and other environmental elements that affect the robot's interaction with the simulation. Having repeatability in a simulated world is important for debugging and testing purposes, for this reason a Python script was used to generate easy to configure worlds from a YAML configuration file. An example of the config file is shown in [Listing A.1](#). For reproducibility, a seed value is configured in the simulation settings, the weed infestation pattern is defined within quadrants of specified dimensions (`quadrant_size`) and each quadrant is individually configured with:

- Spatial distribution:
 - *uniform*: Random uniform distribution
 - *clustered*: Random normal distribution with definable standard deviations (σ_x, σ_y)
- Weed density: Weeds per square meter (weeds/m²)
- Direction: Propagation axis for adjacent quadrants ($\pm x, \pm y$)
- Workspace expansion: If `outside_workspace` is true, the infestation area extends 10% beyond the quadrant boundaries.

A visual result of the generated world using such configuration file is shown in [Figure 3.4](#).



Figure 3.4: Weed Infestation Example

3.2.3 Gazebo Plugins

The files `nuga_gazebo` and `sensors_gazebo` from [Figure 3.3a](#) instantiate and configure Gazebo plugins to define sensor behavior, including optical properties for the camera, as well as update rates and noise models for the IMU and GPS. The file `nuga_ros2_control` on the other hand, establishes an interface between the `IT`'s joints and `ros2_control` framework, specifying the command interface (position), controller type (forward position controller), and movement limits, enabling 3-DOF prismatic motion for each tool. Regarding movement control of the Nuga vehicle, the `ros_planar_move` plugin satisfied all control requirements given the platform's kinematic constraints, eliminating the need for additional configuration.

3.2.4 Joint Control

The control of both `IT` units was handled using the `ros2_control` framework (configuration example shown in [Listing A.2](#)), as previously described. This framework provides a seamless transition between simulation and real hardware control. In this context, the `forward_command_controller` was used, which is recommended for simulation because it bypasses PID computations by directly sending commands to simulated joints. These joints already track positions perfectly, without the disturbances or error correction needed in real-world scenarios. Simulators like Gazebo inherently handle ideal position tracking, making closed-loop control redundant. However, when switching to real hardware, replacing it with a `position_controller` is needed but straightforward thanks to the flexibility of the framework.

Nuga's workspace layout and dimensions are shown in [Figure 3.5](#). The gantry carrying the `IT` operates within a zone of 2.09 m in the `Y` direction, 0.72 m in `X`, and 0.26 m in `Z`. An extraction cycle begins with the gantry moving in `X` and `Y` to position the tool above the plant, followed by a downward movement in `Z` to lower the drill and

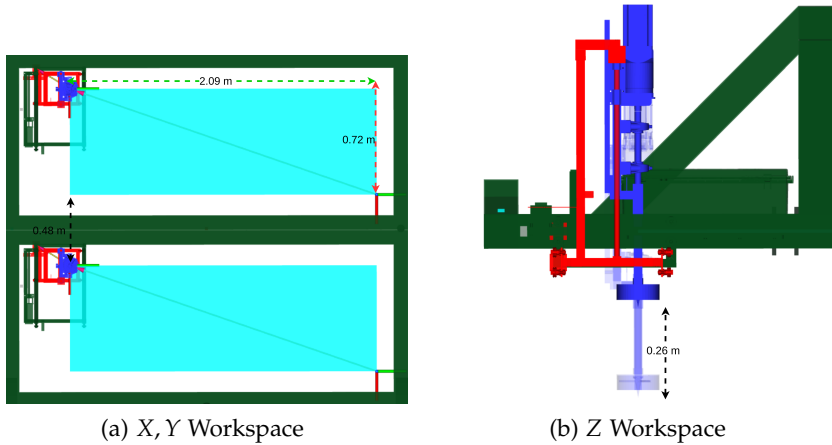


Figure 3.5: IT Workspace Layout

perform the extraction. The gantry has a maximum speed of $1\frac{m}{s}$ in the XY plane, and each extraction can take up to 45 seconds per plant.

The IT is controlled using ROS2 actions, which provide a structured way to handle asynchronous tasks with feedback and result reporting. For the XY movement of the gantry, the AxisPosition action is used, allowing the specification of target coordinates (x, y) and speed, while providing feedback on the current position and confirming whether the target was reached. The Extraction action manages the vertical movement of the tool along the Z axis, reporting the depth reached, total time taken, and success status, along with real-time feedback on the current depth. Finally, the ExtractionCycle action coordinates the execution of multiple extractions by accepting an array of target poses and their corresponding IDs, providing feedback on the current status and reporting the results of the extraction process for each pose. These actions enable precise and modular control of the gantry system, ensuring efficient and reliable operation. A diagram summarizing this process is shown in Figure 3.6.

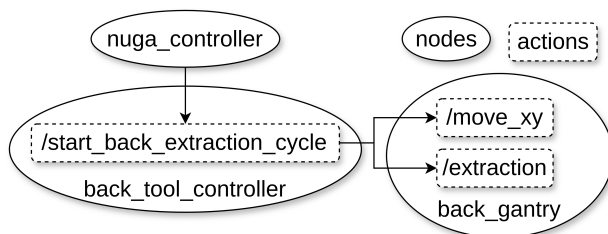


Figure 3.6: ROS Interface for back gantry control

3.2.5 Localization

Accurate localization is essential for mobile robot navigation. In most robotic systems, a combination of sensors such as wheel encoders, IMU's, and GPS (for outdoor applications) are used to estimate the robot's pose in the environment. In simulation, these sensors can be approximated to real-world conditions and provide a testbed for validating higher-level behaviours (e.g., path planning, task allocation, etc.). In this work, the `robot_localization`⁴ package was used to estimate the robot's pose by fusing sensor data. Typically, this would involve:

- An **Extended Kalman Filter (EKF)** fusing high-frequency wheel odometry and IMU data with low-frequency GPS.
- A `navsat_transform_node` to convert GPS data into the robot's odom frame.

However, as wheel odometry was not implemented in the simulation due to plugin limitations, the navigation was done merely using fusion of GPS and IMU, this allowed the EKF to still function and produce a pose estimate. While this approach deviates from standard practice, it was deemed acceptable for this thesis for several reasons: Localization is not the primary contribution of this work, the fused GPS and IMU data provided sufficient accuracy and stability for validating the TA investigation, and the use of `robot_localization` still maintains a realistic pipeline for future extension of real-world deployment.

This setup does not model short-term drift correction that would normally be provided by wheel odometry, and the reliance on GPS alone may introduce small jumps or inaccuracies in pose estimation. These limitations are acknowledged but do not affect the core objectives or validity of the experiments conducted in this work.

3.2.6 Weed Detection

Paltech uses an in-house machine learning model for Rumex recognition, trained on a dataset of images captured under various lighting conditions. The model is integrated into the simulation using a ROS2 node that subscribes to the camera topic and publishes detection results. This node processes camera images, applies the trained model, and outputs the detected plants' positions in camera coordinates along with confidence scores. This integration enables real-time detection of

⁴ `robot_localization` is a collection of state estimation nodes, each of which is an implementation of a nonlinear state estimator for robots moving in 3D space. It contains two state estimation nodes, `ekf_localization_node` and `ukf_localization_node`. In addition, it provides `navsat_transform_node`, which aids in the integration of GPS data. https://docs.ros.org/en/melodic/api/robot_localization/html/index.html

Rumex within the simulated environment, supporting planning and execution of extraction tasks. The model's training dataset includes images such as the one shown in [Figure 3.7a](#), and it is capable of generalizing to simulation images, as illustrated in [Figure 3.7b](#).

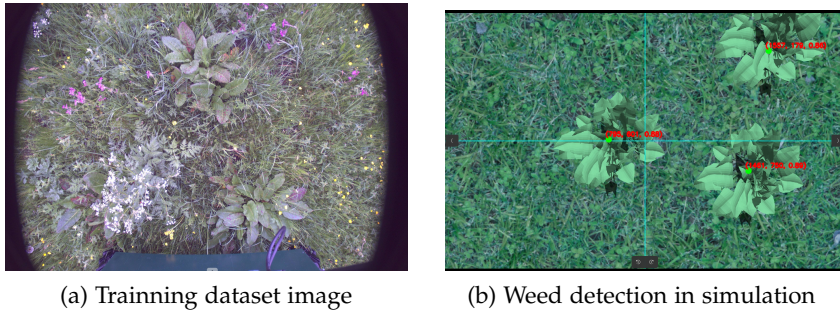


[Figure 3.7: Example of training and detection](#)

3.2.7 Nuga Controller

The Nuga controller is the main node responsible for orchestrating the movement of the robot, managing the [IT](#) units, and performing task allocation based on the weed positions received from the detection node. A high-level overview of the controller's operation is shown in [Figure 3.8](#). The timer callbacks `get_ws_limits()` and `get_imp_offsets()` are self-destructive timers used to retrieve the positions of the tool workspace limits and their offsets relative to the `base_link`. Once this information is received, the timers are destroyed. The same applies to the callback of the `/head_camera/camera_info` topic, which is used to obtain the camera's central pixel position for later use.

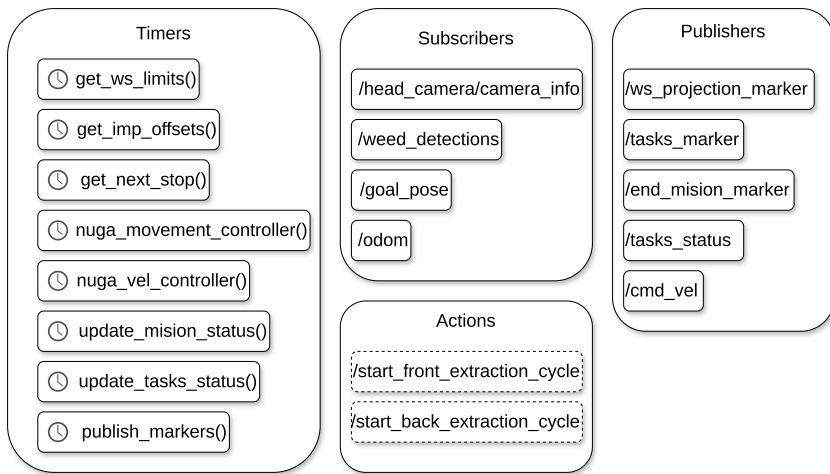


[Figure 3.8: Nuga Controller ROS Interface](#)

The `get_next_stop()` function is a timer callback that computes the robot's next stop when required. It uses the current detections, the

robot's pose, and the selected task allocation algorithm to determine the next target position, as well as the tasks to be executed at that stop by each IT. The execution steps followed by this method are shown in Algorithm 5.

Once a stop is determined, Nuga's movement and velocity controllers govern the robot's behavior. The `nuga_movement_controller()` function switches the robot's state between *stationary* and *moving* when needed, while also measuring the time spent in each state. If the robot reaches the target position, this method stops the robot and triggers the actions required to perform the extraction cycle; otherwise, it keeps the robot in the *moving* state. Finally, `nuga_velocity_controller()` takes the robot's state and computes the necessary velocity commands, publishing them to the `/cmd_vel` topic.

The callback `update_mission_status()` continuously checks whether the robot has reached the end-of-mission position in order to stop it and generate log information for mission metrics. On the other hand, `update_tasks_status()` continuously publishes the status of all weed detections to the `/tasks_status` topic. These tasks can include those assigned to the back or front tool, current detections, tasks outside the future path, and failed tasks.

Finally, `publish_markers()` updates RViz markers to visualize robot position and task status. Figure 3.9 shows an example of the RViz visualization in a usual mission.

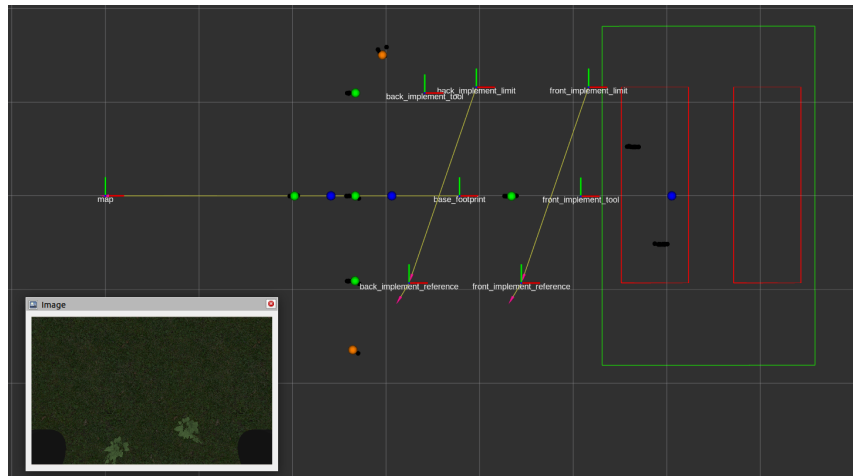


Figure 3.9: RViz Visualization

FIGURE 3.9 Displays the current position of the robot (`base_link`), the tool workspaces, and tool positions using coordinate frames. Task categories are indicated with colored spheres: green for successful tasks, orange for tasks outside the path, red for failed tasks, and blue for robot stops. The workspace projections of the onboard tools are shown using red rectangles, while the green rectangle represents the front camera's field of view.

3.3 TASK ALLOCATION

Paltech currently offers its weeding solutions in fields ranging from 0.5 to 20 hectares, with an average weed density of 0.4 to 2.0 weeds/m². [Figure 3.10a](#) shows an example of usual weed density in a 1-hectare field, while [Figure 3.10b](#) illustrates the coverage path planning pattern that the robot follows in the same field. The simulations in this thesis are limited to the linear movements shown in [3.10b](#), due to the motion constraints described at the beginning of [Section 2.1](#). As a result, the simulation environments were designed accordingly.

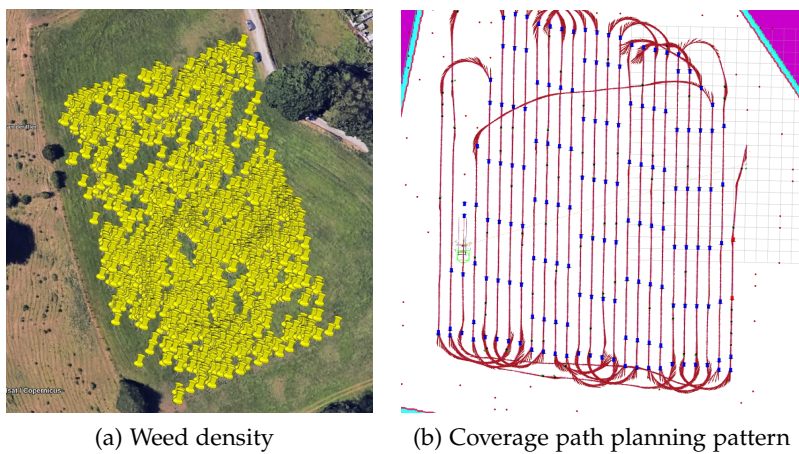


Figure 3.10: Weed distribution and coverage path in an agricultural field

3.3.1 Simulation Setup

Simulations were customized using YAML files, as mentioned in [Section 3.2](#), allowing for ease of configuration and logging convenience. All tests took place in a rectangular grass field of 10m × 50m, with different weed densities along a straight strip of 2m × 50m, simulating one line of the coverage path planning (observe an example in [Figure 3.11](#)). The local weed distribution within each quadrant (2m × 2m) varied in both type (*uniform* or *clustered*) and density, replicating irregular Rumex growth.

3.3.2 Algorithm Comparison

The first simulation corresponds to an infestation area of 100m², with a weed density of 0.28 weeds/m². This simulates a low weed density scenario, as shown in [Figure 3.12a](#). [Figure 3.12](#) presents both the task visualization and the mission metrics comparison across algorithms.

The first two missions in [Figure 3.12b](#) represent the baseline method using one and two tools, respectively. This comparison was made only to determine the natural improvement in mission time when adding

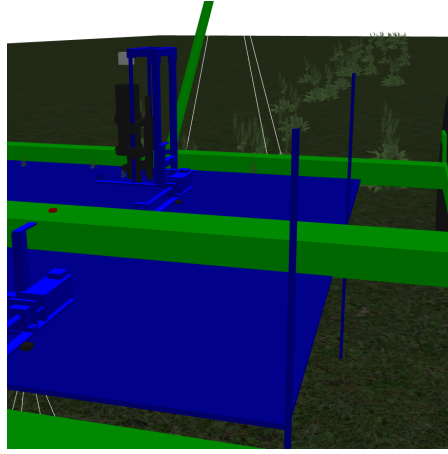


Figure 3.11: Simulation Example

an additional tool, even with a non-optimized algorithm. Missions three, four, and five correspond to the graph search, optimization, and market-based approaches, respectively. We observe similar mission times and no significant improvement over the baseline method, which is expected since the weed density is low and, most of the time, the separation between weeds prevents the robot from reaching them with both tools simultaneously. Nevertheless, we observe a reduction in tool idle time with algorithms three, four, and five. The heuristic algorithm results in an idle time of 12.8 min. for the front tool, whereas the others remain within the range of 8 min. to 9.8 min.

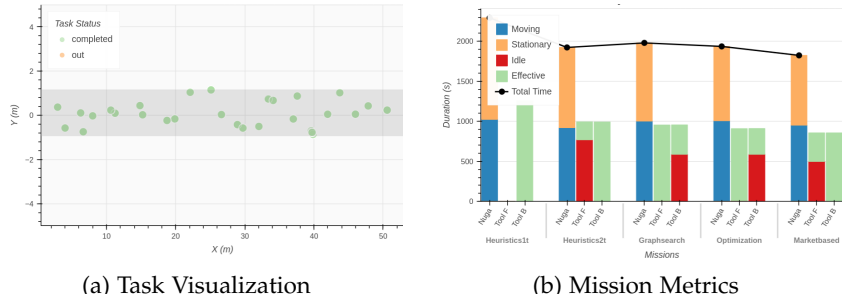


Figure 3.12: Low density algorithms comparison

For the second simulation, we increased the average weed density to 0.55 weeds/m², simulating a medium-density scenario, as shown in Figure 3.13a. In Figure 3.13b, we observe improvements in both mission time and tool productivity. Both the graph search and optimization-based algorithms show improvements compared to the heuristic approach. Specifically, while the baseline method overuses the back tool, resulting in high idle time for the front tool, graph search and optimization achieve more balanced tool usage. The market-based algorithm also reduces idle time, although not as significantly as the other two methods.

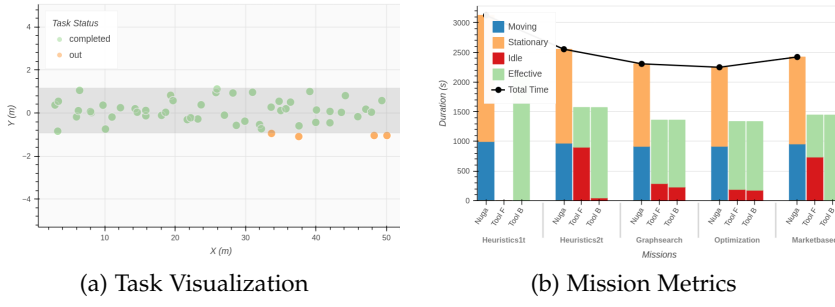


Figure 3.13: Medium density algorithms comparison

The third simulation corresponds to a weed density of 1.55 weeds/m², simulating a high-density scenario, as shown in Figure 3.14a. Similar to the medium-density scenario (but more pronounced) the graph search and optimization-based approaches show better performance by reducing both mission time and idle time for both tools, achieving balanced tool usage. The market-based algorithm also shows noticeable improvements, achieving better tool productivity and mission time reduction than the baseline, although it still lags behind the other two methods.

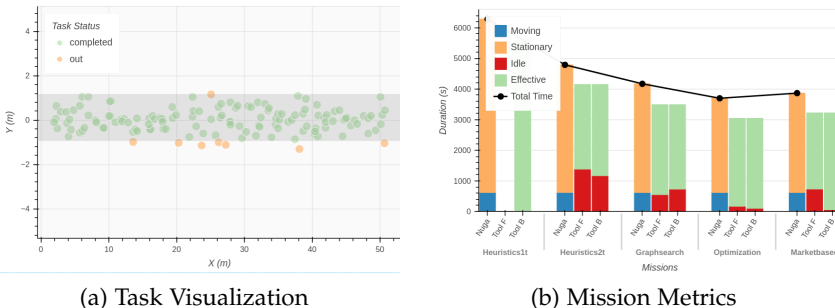


Figure 3.14: High density algorithms comparison

The simulation results are summarized in Table 3.1, Table 3.2, Table 3.3 for the low, medium, and high-density simulations, respectively. Each table presents the same information as the previous bar graphs under the 'Raw' column. Additionally, the 'Improvement' column shows the relative percentage difference of each algorithm compared to the baseline method for each category. This allows to determine the best algorithm for each weed density scenario.

		Raw (min)						Improvement (%)					
		Mov.	Stat.	Total	Idle	Eff.	Mov.	Stat.	Total	Idle	Eff.		
Market	Heuristics	N	15.3	16.7	32	-	-	-	-	-	-	-	-
		FT	-	-	-	12.8	3.7	-	-	-	-	-	-
		BT	-	-	-	0.1	16.4	-	-	-	-	-	-
	Graph Search	N	16.7	16.2	32.9	-	-	9.2	-3.0	2.8	-	-	-
		FT	-	-	-	0.1	15.7	-	-	-	-99.2	324.3	
	BT	-	-	-	-	9.8	6.1	-	-	-	9700.0	-62.8	
Optimization	Heuristics	N	16.7	15.4	32.2	-	-	9.2	-7.8	0.6	-	-	-
		FT	-	-	-	0.1	14.9	-	-	-	-99.2	302.7	
		BT	-	-	-	9.8	5.3	-	-	-	9700.0	-67.7	
	Graph Search	N	15.8	14.5	30.3	-	-	3.3	-13.2	-5.3	-	-	-
		FT	-	-	-	8.3	5.9	-	-	-	-35.2	59.5	
	BT	-	-	-	-	0.1	14.2	-	-	-	0.0	-13.4	

Table 3.1: Low-density Simulation Results

TABLE 3.1 Confirms that there is no significant improvement in mission time nor tool productivity when using more sophisticated algorithms in low-density scenarios. We observe that the market-based approach was the only one to achieve a reduction in total mission time, with a 5.3% decrease compared to the baseline method. In contrast, the graph search and optimization methods actually increased the mission time by 2.8% and 0.6%, respectively.

Regarding tool productivity, we observe a shift in which tool experiences more idle time: from the front tool in the baseline to the back tool in the cases of graph search and optimization. Despite this shift, both methods reduced the back tool’s idle time from 12.8 minutes to 9.8 minutes. The market-based method maintained the front tool as the one with the highest idle time but still achieved a 35.2% reduction.

			Raw (min)						Improvement (%)					
			Mov.	Stat.	Total	Idle	Eff.	Mov.	Stat.	Total	Idle	Eff.		
Graph Search	Heuristics	N	16.1	26.4	42.5	-	-	-	-	-	-	-	-	-
		FT	-	-	-	15	11.1	-	-	-	-	-	-	-
		BT	-	-	-	0.7	25.3	-	-	-	-	-	-	-
	Optimization	N	15.2	23.1	38.4	-	-	-5.6	-12.5	-9.6	-	-	-	-
		FT	-	-	-	4.8	17.8	-	-	-	-	-68.0	60.4	
		BT	-	-	-	3.8	18.8	-	-	-	-	442.9	-25.7	
Market	Heuristics	N	16	24.5	40.6	-	-	-0.6	-7.2	-4.5	-	-	-	-
		FT	-	-	-	1.7	22.4	-	-	-	-	-88.7	101.8	
		BT	-	-	-	9.8	14.2	-	-	-	-	1300.0	-43.9	
	Optimization	N	15.9	24.4	40.3	-	-	-1.2	-7.6	-5.2	-	-	-	-
		FT	-	-	-	12.2	11.8	-	-	-	-	-18.7	6.3	
		BT	-	-	-	0	24	-	-	-	-	-100.0	-5.1	

Table 3.2: Medium-density Simulation Results

			Raw (min)						Improvement (%)					
			Mov.	Stat.	Total	Idle	Eff.	Mov.	Stat.	Total	Idle	Eff.		
Graph Search	Heuristics	N	10.3	69.4	79.8	-	-	-	-	-	-	-	-	-
		FT	-	-	-	23	46	-	-	-	-	-	-	-
		BT	-	-	-	19.5	49.6	-	-	-	-	-	-	-
	Optimization	N	10.3	59.1	69.4	-	-	0.0	-14.8	-13.0	-	-	-	-
		FT	-	-	-	9.1	48.9	-	-	-	-	-60.4	6.3	
		BT	-	-	-	12.1	45.9	-	-	-	-	-37.9	-7.5	
Market	Heuristics	N	10.3	51.2	61.6	-	-	0.0	-26.2	-22.8	-	-	-	-
		FT	-	-	-	2.8	47.8	-	-	-	-	-87.8	3.9	
		BT	-	-	-	1.7	48.9	-	-	-	-	-91.3	-1.4	
	Optimization	N	10.3	54	64.4	-	-	0.0	-22.2	-19.3	-	-	-	-
		FT	-	-	-	12.2	41.4	-	-	-	-	-47.0	-10.0	
		BT	-	-	-	1	52.6	-	-	-	-	-94.9	6.0	

Table 3.3: High-density Simulation Results

TABLE 3.2 Highlights the improvements achieved in medium-density scenarios by the implemented algorithms over the heuristic approach. The graph search, optimization, and market-based methods reduced mission time by 9.6%, 4.5%, and 5.2%, respectively. Additionally, they achieved more balanced tool usage and reductions in idle time up to 88.7% for the front tool. The observed increment in back tool idle time is attributed to the heuristic method’s unbalanced tool usage, which resulted in a very low idle time for only one tool, which is not desired.

TABLE 3.3 Demonstrates the effectiveness of the proposed algorithms in high-density scenarios. The graph search, optimization, and market-based methods achieved mission time reductions of 13.0%, 22.8%, and 19.3%, respectively. In terms of tool usage, all three methods achieved a balanced tool usage, with reductions in idle time of up to 87.8% for the front tool and up to 94.9% for the back tool.

3.3.3 Computation Time

The heuristic and market-based algorithms are considered short-sighted in nature due to the way they compute the next best stop without considering all tasks available up to that point. This characteristic makes their computation time negligible, regardless of the number of tasks currently available. In contrast, graph search and optimization-based algorithms take all available information into account when computing a solution, resulting in a larger solution space and, consequently, greater computational effort.

Our graph search solution performs well in terms of computation time, for a low to medium density of weeds. However, as the number of weeds increases, the graph size grows exponentially, leading to longer computation times. [Figure 3.15](#) showcases the graph size and computation time for different number of weeds (see plot in red). The graph size is defined as the number of nodes in the graph, while the computation time is the time required to build and find the optimal path in the graph.

We were able to optimize and reduce the graph size by applying a pruning technique that stops the growth of certain branches when they are not promising. This is achieved by introducing the concept of *expired tasks*, these are tasks that haven’t been removed and can no longer be removed in future stops because the corresponding weeds have been left behind, outside the tool’s workspaces. This pruning is implemented in the `get_children_nodes` method, where each task is checked for expiration before being added to the graph. As a result, the number of nodes is significantly reduced, improving computation time (observe green plot in [Figure 3.15](#)).

A similar computation time analysis was done for the optimization-based algorithm, and the comparison between them is shown in FX.

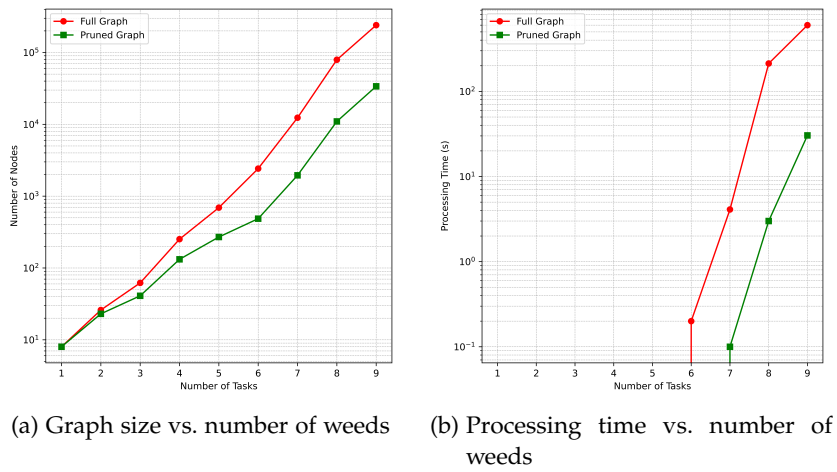


Figure 3.15: Graph Search algorithm performance

3.3.4 Future Work

4

CONCLUSIONS

A

APPENDIX

A.1 CONFIGURATION FILES

YAML files are the standard method for setting up configuration variables in the Nuga project. A collection of configuration examples is provided in this appendix.

Listing A.1: Weed Infestation World config example

```
seed: 2
quadrant_size: [2.0, 2.0]
quadrants:
  1:
    direction: x
    weed_density: 0.4    # weeds/m2
    spatial_distribution: clustered
    std_dev: [0.5, 0.5]
    outside_workspace: false
  2:
    direction: x
    weed_density: 1.2    # weeds/m2
    spatial_distribution: uniform
    outside_workspace: false
```

Listing A.2: ROS2 config example

```
# ROS2 Control
controller_manager:
  ros__parameters:
    use_sim_time: True
    update_rate: 20 # Hz

  joint_state_broadcaster:
    type: joint_state_broadcaster/JointStateBroadcaster

  forward_position_controller_front:
    type: forward_command_controller/ForwardCommandController
forward_position_controller_front:
  ros__parameters:
    joints:
      - front_x_axis_joint
      - front_y_axis_joint
      - front_implement_tool_joint
  interface_name: position
```

A.2 ALGORITHMS

Algorithm 4 Depth-First Search

Require: *root_node, last_node*

Ensure: Explored Graph

```

1: visited ← {last_node} {Initialize with last node}
2: stack ← [root_node] {Start with root node}
3: i ← 0 {Iteration counter}
4: while stack is not empty do
5:   i ← i + 1
6:   node ← stack.pop()
7:   if node ∉ visited then
8:     visited.add(node)
9:     children ← get_children_nodes(node)
10:    if children ≠ None then
11:      stack.extend(children) {Add children to stack}
12:    end if
13:  end if
14:  if i == 5000 then
15:    break {Early termination}
16:  end if
17: end while

```

Algorithm 5 Get Next Stop

Require: Detections, Robot pose
Ensure: Next stop pose and assigned tasks

```

1: if stop_pose ≠ None then
2:   return
3: end if
4: if detections is empty then
5:   nuga_state ← "moving"
6:   return
7: end if
8: (tasks_in, tasks_out) ← get_tasks_in_future_path()
9: now ← current_time
10: if tasks_out is not empty then
11:   for all (idx, pose) ∈ tasks_out do
12:     tasks_out_ws[idx] ← pose
13:     add_marker("map", now, "out", idx, pose, "orange")
14:   end for
15: end if
16: if tasks_in is empty then
17:   nuga_state ← "moving"
18:   return
19: end if
20: algorithm.set_robot_pose(nuga_pose)
21: algorithm.set_tasks(tasks_in)
22: (stop_pose, stop_tasks) ← algorithm.compute_next_stop()
23: add_marker("map", now, "goal", stops_counter + 1,
24:           stop_pose, "blue")
25: clear_polygons()
26: id ← 0
27: for all (name, imp) ∈ implements do
28:   add_polygon("map", now, name + "_ws", id,
29:             imp.future_ws_pose)
30:   id ← id + 1
31: end for
  
```

BIBLIOGRAPHY

- [1] T. Zhang, Q. Li, Cs. Zhang, et al. "Current trends in the development of intelligent unmanned autonomous systems." In: *Frontiers in Information Technology & Electronic Engineering* 18 (2017), pp. 68–85. DOI: [10.1631/FITEE.1601650](https://doi.org/10.1631/FITEE.1601650).
- [2] Klötzli J., Suter M., Beaumont D. and Kolmanic A., Leskovsek R., and Schaffner U. "Key management practices to reduce the risk of the occurrence of Rumex obtusifolius in productive grasslands." In: *Weed Research* 1.64 (2021), pp. 76–88.
- [3] Mueller C., Sroka L., Hass M.L., Aboling S., These A., and Vervuert I. "Rejection behaviour of horses for hay contaminated with meadow saffron Colchicum autumnale L." In: *Journal of Animal Physiology and Animal Nutrition* 1.106 (2022), pp. 327–334.
- [4] Athira K A, Divya Udayan J, and Umashankar Subramaniam. "A Systematic Literature Review on Multi-Robot Task Allocation." In: *ACM Comput. Surv.* 57.3 (Nov. 2024). ISSN: 0360-0300. DOI: [10.1145/3700591](https://doi.org/10.1145/3700591). URL: <https://doi.org/10.1145/3700591>.
- [5] Javier G. Martin, Francisco Javier Muros, José María Maestre, and Eduardo F. Camacho. "Multi-robot task allocation clustering based on game theory." In: *Robotics and Autonomous Systems* 161 (2023), p. 104314. ISSN: 0921-8890. DOI: <https://doi.org/10.1016/j.robot.2022.104314>. URL: <https://www.sciencedirect.com/science/article/pii/S0921889022002032>.
- [6] Junyan Hu, Parijat Bhowmick, Inmo Jang, Farshad Arvin, and Alexander Lanzon. "A Decentralized Cluster Formation Containment Framework for Multirobot Systems." In: *IEEE Transactions on Robotics* 37.6 (2021), pp. 1936–1955. DOI: [10.1109/TRO.2021.3071615](https://doi.org/10.1109/TRO.2021.3071615).
- [7] Xinye Chen, Ping Zhang, Fang Li, and Guanglong Du. "A cluster first strategy for distributed multi-robot task allocation problem with time constraints." In: *2018 WRC Symposium on Advanced Robotics and Automation (WRC SARA)*. 2018, pp. 102–107. DOI: [10.1109/WRC-SARA.2018.8584210](https://doi.org/10.1109/WRC-SARA.2018.8584210).
- [8] Jeongeon Kim and Hyoung Il Son. "A Voronoi Diagram-Based Workspace Partition for Weak Cooperation of Multi-Robot System in Orchard." In: *IEEE Access* 8 (2020), pp. 20676–20686. DOI: [10.1109/ACCESS.2020.2969449](https://doi.org/10.1109/ACCESS.2020.2969449).

- [9] Darren Smith, Jodie Wetherall, Stephen Woodhead, and Andrew Adekunle. "A Cluster-Based Approach to Consensus Based Distributed Task Allocation." In: *2014 22nd Euromicro International Conference on Parallel, Distributed, and Network-Based Processing*. 2014, pp. 428–431. DOI: [10.1109/PDP.2014.87](https://doi.org/10.1109/PDP.2014.87).
- [10] Qi Lu, Joshua P. Hecker, and Melanie E. Moses. "Multiple-place swarm foraging with dynamic depots." In: *Autonomous Robots* 42.4 (2018), pp. 909–926. DOI: [10.1007/s10514-017-9693-2](https://doi.org/10.1007/s10514-017-9693-2). URL: <https://doi.org/10.1007/s10514-017-9693-2>.
- [11] Jiamei Lin, Pengcheng Li, Jialong Dai, Shaorui Liu, Wei Tian, Bo Li, and Changrui Wang. "Multi-robot Cooperative Assembly Task Planning for Large-scale Aerospace Structures." In: *2022 37th Youth Academic Annual Conference of Chinese Association of Automation (YAC)*. 2022, pp. 795–800. DOI: [10.1109/YAC57282.2022.10023897](https://doi.org/10.1109/YAC57282.2022.10023897).
- [12] Shiguang Wu, Xiaojie Liu, Xingwei Wang, Xiaolin Zhou, and Mingyang Sun. "Multi-robot Dynamic Task Allocation Based on Improved Auction Algorithm." In: *2021 6th International Conference on Automation, Control and Robotics Engineering (CACRE)*. 2021, pp. 57–61. DOI: [10.1109/CACRE52464.2021.9501305](https://doi.org/10.1109/CACRE52464.2021.9501305).
- [13] Dong-Hyun Lee, Sheir Afgen Zaheer, Ji-Hyeong Han, Jong hwan Kim, and Eric Matson. "Competency adjustment and workload balancing framework in multirobot task allocation." In: *International Journal of Advanced Robotic Systems* 15.6 (2018), p. 1729881418812960. DOI: [10.1177/1729881418812960](https://doi.org/10.1177/1729881418812960). URL: <https://doi.org/10.1177/1729881418812960>.
- [14] Andong Shi, Shilei Cheng, Lei Sun, and Jingtai Liu. "Multi-robot Task Allocation for Airfield Pavement Detection Tasks." In: *2021 6th International Conference on Control, Robotics and Cybernetics (CRC)*. 2021, pp. 62–67. DOI: [10.1109/CRC52766.2021.9620140](https://doi.org/10.1109/CRC52766.2021.9620140).
- [15] Dong-Hyun Lee, Sheir Afgen Zaheer, and Jong-Hwan Kim. "A Resource-Oriented, Decentralized Auction Algorithm for Multirobot Task Allocation." In: *IEEE Transactions on Automation Science and Engineering* 12.4 (2015), pp. 1469–1481. DOI: [10.1109/TASE.2014.2361334](https://doi.org/10.1109/TASE.2014.2361334).
- [16] Gautham P. Das, Thomas M. McGinnity, Sonya A. Coleman, and Laxmidhar Behera. "A Distributed Task Allocation Algorithm for a Multi-Robot System in Healthcare Facilities." In: *Journal of Intelligent & Robotic Systems* 80.1 (2015), pp. 33–58. DOI: [10.1007/s10846-014-0154-2](https://doi.org/10.1007/s10846-014-0154-2). URL: <https://doi.org/10.1007/s10846-014-0154-2>.
- [17] Lingzhi Luo, Nilanjan Chakraborty, and Katia Sycara. "Distributed algorithm design for multi-robot task assignment with deadlines for tasks." In: *2013 IEEE International Conference on*

- Robotics and Automation*. 2013, pp. 3007–3013. DOI: [10.1109/ICRA.2013.6630994](https://doi.org/10.1109/ICRA.2013.6630994).
- [18] Xingjie Liu, Guolei Wang, and Ken Chen. “Option-Based Multi-Agent Reinforcement Learning for Painting With Multiple Large-Sized Robots.” In: *IEEE Transactions on Intelligent Transportation Systems* 23.9 (2022), pp. 15707–15715. DOI: [10.1109/TITS.2022.3145375](https://doi.org/10.1109/TITS.2022.3145375).
 - [19] Ahmed Elfakharany and Zool Hilmi Ismail. “End-to-End Deep Reinforcement Learning for Decentralized Task Allocation and Navigation for a Multi-Robot System.” In: *Applied Sciences* 11.7 (2021). ISSN: 2076-3417. DOI: [10.3390/app11072895](https://doi.org/10.3390/app11072895). URL: <https://www.mdpi.com/2076-3417/11/7/2895>.
 - [20] Zheyuan Wang, Chen Liu, and Matthew Gombolay. “Heterogeneous Graph Attention Networks for Scalable Multi-Robot Scheduling with Temporospatial Constraints.” In: *Autonomous Robots* 46.1 (2022), pp. 249–268. DOI: [10.1007/s10514-021-09997-2](https://doi.org/10.1007/s10514-021-09997-2). URL: <https://doi.org/10.1007/s10514-021-09997-2>.
 - [21] Steve Paul, Payam Ghassemi, and Souma Chowdhury. *Learning Scalable Policies over Graphs for Multi-Robot Task Allocation using Capsule Attention Networks*. 2022. arXiv: [2205.03321 \[cs.MA\]](https://arxiv.org/abs/2205.03321). URL: <https://arxiv.org/abs/2205.03321>.
 - [22] Bumjin Park, Cheongwoong Kang, and Jaesik Choi. “Cooperative Multi-Robot Task Allocation with Reinforcement Learning.” In: *Applied Sciences* 12.1 (2022). ISSN: 2076-3417. DOI: [10.3390/app12010272](https://doi.org/10.3390/app12010272). URL: <https://www.mdpi.com/2076-3417/12/1/272>.
 - [23] Jacopo Banfi, Andrew Messing, Christopher Kroninger, Ethan Stump, Seth Hutchinson, and Nicholas Roy. “Hierarchical Planning for Heterogeneous Multi-Robot Routing Problems via Learned Subteam Performance.” In: *IEEE Robotics and Automation Letters* 7.2 (2022), pp. 4464–4471. DOI: [10.1109/LRA.2022.3148489](https://doi.org/10.1109/LRA.2022.3148489).
 - [24] Gennaro Notomista, Siddharth Mayya, Yousef Emam, Christopher Kroninger, Addison Bohannon, Seth Hutchinson, and Magnus Egerstedt. “A Resilient and Energy-Aware Task Allocation Framework for Heterogeneous Multirobot Systems.” In: *IEEE Transactions on Robotics* 38.1 (2022), pp. 159–179. DOI: [10.1109/TRO.2021.3102379](https://doi.org/10.1109/TRO.2021.3102379).
 - [25] Nicholas Lindsay, Robert K. Buehling, and Lihong Sun. “A Sequential Task Addition Distributed Assignment Algorithm for Multi-Robot Systems.” In: *Journal of Intelligent & Robotic Systems* 102 (2021), p. 51. DOI: [10.1007/s10846-021-01394-7](https://doi.org/10.1007/s10846-021-01394-7).

- [26] Zhi Li, Ali Vatankhah Barenji, Jiazhi Jiang, Ray Y. Zhong, and Gangyan Xu. "A Mechanism for Scheduling Multi Robot Intelligent Warehouse System Face with Dynamic Demand." In: *Journal of Intelligent Manufacturing* 31.2 (2020), pp. 469–480. DOI: [10.1007/s10845-018-1459-y](https://doi.org/10.1007/s10845-018-1459-y). URL: <https://doi.org/10.1007/s10845-018-1459-y>.
- [27] Shridhar Velhal, Suresh Sundaram, and Narasimhan Sundararajan. "Dynamic Resource Allocation With Decentralized Multi-Task Assignment Approach for Perimeter Defense Problem." In: *IEEE Transactions on Aerospace and Electronic Systems* 58.4 (2022), pp. 3313–3325. DOI: [10.1109/TAES.2022.3147742](https://doi.org/10.1109/TAES.2022.3147742).
- [28] Siddharth Mayya, Diego S. D'antonio, David Saldaña, and Vijay Kumar. *Resilient Task Allocation in Heterogeneous Multi-Robot Systems*. 2021. arXiv: [2009.04593 \[cs.MA\]](https://arxiv.org/abs/2009.04593). URL: <https://arxiv.org/abs/2009.04593>.
- [29] Kelin Jose and Dilip Kumar Pratihar. "Task allocation and collision-free path planning of centralized multi-robots system for industrial plant inspection using heuristic methods." In: *Robotics and Autonomous Systems* 80 (2016), pp. 34–42. ISSN: 0921-8890. DOI: <https://doi.org/10.1016/j.robot.2016.02.003>. URL: <https://www.sciencedirect.com/science/article/pii/S0921889016000282>.
- [30] Gennaro Notomista, Siddharth Mayya, Seth Hutchinson, and Magnus Egerstedt. *An Optimal Task Allocation Strategy for Heterogeneous Multi-Robot Systems*. 2019. arXiv: [1903.08641 \[cs.R0\]](https://arxiv.org/abs/1903.08641). URL: <https://arxiv.org/abs/1903.08641>.
- [31] Wanqing Zhao, Qinggang Meng, and Paul W. H. Chung. "A Heuristic Distributed Task Allocation Method for Multivehicle Multitask Problems and Its Application to Search and Rescue Scenario." In: *IEEE Transactions on Cybernetics* 46.4 (2016), pp. 902–915. DOI: [10.1109/TCYB.2015.2418052](https://doi.org/10.1109/TCYB.2015.2418052).
- [32] Oscar Valero, Javier Antich, Antoni Tauler-Rosselló, José Guerrero, Juan-José Miñana, and Alberto Ortiz. "Multi-robot task allocation methods: A fuzzy optimization approach." In: *Information Sciences* 648 (2023), p. 119508. ISSN: 0020-0255. DOI: <https://doi.org/10.1016/j.ins.2023.119508>. URL: <https://www.sciencedirect.com/science/article/pii/S0020025523010939>.
- [33] Robert Tarjan. "Depth-First Search and Linear Graph Algorithms." In: *SIAM Journal on Computing* 1.2 (1972), pp. 146–160. DOI: [10.1137/0201010](https://doi.org/10.1137/0201010). eprint: <https://doi.org/10.1137/0201010>. URL: <https://doi.org/10.1137/0201010>.

- [34] E. W. Dijkstra. “A Note on Two Problems in Connexion with Graphs.” In: *Numerische Mathematik* 1.1 (1959), pp. 269–271.
DOI: [10.1007/BF01386390](https://doi.org/10.1007/BF01386390). URL: <https://doi.org/10.1007/BF01386390>.

DECLARATION

Put your declaration here.

Zagreb, Croatia, June 2025

David Raziel Ceres Arroyo

COLOPHON

This document was typeset using the typographical look-and-feel `classicthesis` developed by André Miede and Ivo Pletikosić. The style was inspired by Robert Bringhurst's seminal book on typography "*The Elements of Typographic Style*". `classicthesis` is available for both L^AT_EX and L^YX:

<https://bitbucket.org/amiede/classicthesis/>

Happy users of `classicthesis` usually send a real postcard to the author, a collection of postcards received so far is featured here:

<http://postcards.miede.de/>

Thank you very much for your feedback and contribution.